ISSN 1674-1056
http://cpb.iphy.ac.cn
http://iopscience.iop.org/cpb
中国物理 B
Chinese Physics
中国物理
Chinese Physics B

Dynamic nucleation of domain-chains in magnetic nanotracks

Xiangjun Jin(金香君), Yong Li(李勇), Fusheng Ma(马付胜)

Citation: Chin. Phys. B . 2018, 27(12): 127504. **doi:** 10.1088/1674-1056/27/12/127504

What follows is a list of articles you may be interested in

Interfacial effect on the reverse of magnetization and ultrafast demagnetization in Co/Ni bilayers with perpendicular magnetic anisotropy

Zi-Zhao Gong(弓子召), Wei Zhang(张伟), Wei He(何为), Xiang-Qun Zhang(张向群), Yong Liu(刘永), Zhao-Hua Cheng(成昭华)

Chin. Phys. B . 2018, 27(5): 057501. **doi:** 10.1088/1674-1056/27/5/057501

Effects of dipolar interactions on magnetic properties of Co nanowire arrays

Hong-Jian Li(李洪健), MingYue(岳明), Qiong Wu(吴琼), Yi Peng(彭懿), Yu-Qing Li(李玉卿), Wei-Qiang Liu(刘卫强), Dong-Tao Zhang(张东涛), Jiu-Xing Zhang(张久兴)

Chin. Phys. B . 2017, 26(11): 117503. **doi:** 10.1088/1674-1056/26/11/117503

Faster vortex core switching with lower current density using three-nanocontact spin-polarized currents in a confined structure

Hua-Nan Li(李化南), Zhong Hua(华中), Dong-Fei Li(李东飞)

Chin. Phys. B . 2017, 26(1): 017502. **doi:** 10.1088/1674-1056/26/1/017502

Nonmonotonic effects of perpendicular magnetic anisotropy on current-driven vortex wall motions in magnetic nanostripes

Su Yuan-Chang, Lei Hai-Yang, Hu Jing-Guo

Chin. Phys. B . 2015, 24(9): 097506. **doi:** 10.1088/1674-1056/24/9/097506

Shape-manipulated spin-wave eigenmodes of magnetic nanoelements

Zhang Guang-Fu, Li Zhi-Xiong, Wang Xi-Guang, Nie Yao-Zhuang, Guo Guang-Hua

Chin. Phys. B . 2015, 24(9): 097503. **doi:** 10.1088/1674-1056/24/9/097503

SPECIAL TOPIC — 60th Anniversary of Department of Physics of Nanjing Normal University

Dynamic nucleation of domain-chains in magnetic nanotracks*

Xiangjun Jin(金香君), Yong Li(李勇), and Fusheng Ma(马付胜)†

Center for Quantum Transport and Thermal Energy Science, Magnetoelectronic Laboratory, School of Physics and Technology, Nanjing Normal University, Nanjing 210023, *China*

(Received 30 August 2018; revised manuscript received 16 November 2018; published online 25 November 2018)

Most of the reported observations are about the dynamic properties of individual domain-walls in magnetic nanowires, but the properties of multiple stripe-domains have rarely been investigated. Here, we demonstrate a simple but efficient scenario for multiple domains injection in magnetic nanowires. The domain-chains (DCs), a cluster of multiple domains, can be dynamically generated with tunable static properties. It is found that the number of domains in a single DC can be dynamically adjusted by varying the frequency of microwave field (MF) and the period of spin-polarized current (SPC) intensity. The static properties of the DCs, *i.e.*, its length, spacing, and period between neighboring DCs, can be dynamically controlled by regulating the frequency of MF and the intensity of SPC. We have also discussed the possibility of using domain-chains as information carries, which provides a meaningful approach for flexible multi-bit information storage applications.

Keywords: domain-chains, micromagnetic simulation, domain motion, spin-transfer torque

PACS: 75.78.Fg, 75.75.–c, 75.70.Kw, 75.78.Cd **DOI:** 10.1088/1674-1056/27/12/127504

1. Introduction

With the development of nano-technology, high-density storage becomes an inevitable trend. Compared to the traditional hard disk, the racetrack memory based on magnetic domains (such as domain wall, skyrmion) can greatly improve the storage density. The dynamical behavior of magnetic domain walls[1–3] has been extensively investigated. As previously reported, due to the coupling effect of the antiferromagnetic layer film on the ferromagnetic layer, the magnetic domain wall width and the domain wall moving speed of the system change significantly.[4,5] In such domain wall-based racetrack memories, extensive research has been conducted on how to reduce the critical current density, reduce the influence of the pinning layer, and maintain the high-speed motion of the domain walls.[1,2,6] In particular, the spin-transfer torque (STT) driven motion of magnetic domain-walls and skyrmions has been demonstrated in magnetic nanowires.[7–16] The current-induced DW motion[12,17–20] has attracted much attention, since it provides an alternative candidate as information carries for the next-generation spintronic devices.[10,16,18,21–25] However, most of the research contents are about individual DW. From the application point of view, the multiple domain-based devices have the advances of manipulating flexibility and tunability in magnetic nanostructures.

In this work, we numerically investigated the dynamic nucleation of domain-chains (DCs) in magnetic nanowire using micromagnetic simulations. To distinguish them from isolate domains, we defined domain-chains as clusters comprised of multiple equally spaced domains, *i.e.*, multiple domains forming one chain. The schematic diagram of a domain-chain containing two domains is shown in Fig. 1. Here, for the sake of simplicity, the number of "blue" domains counts the number of domains in each domain-chain. For instance, the dashed box in Fig. 1 shows a domain-chain containing two "blue" color domains with $N = 2$, which will be presented as 2-DC. We numerically proved the continuous creation of DCs and their STT-driven motion in the nanotrack. It is found that the properties of DCs can be manipulated by controlling either the frequency of microwave field (MF) or the period of spin-polarized current (SPC) intensity.

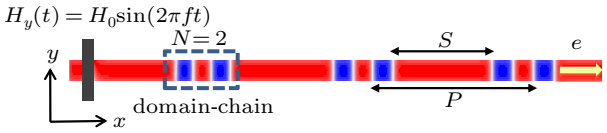


Fig. 1. (color online) Schematic diagram of investigated nanotrack for the nucleation of magnetic domain-chains. An microwave field $H_y(t)$ was locally generated on the left end of the nanotrack by an antenna. The spin-polarized current was applied along the $-x$ direction, and via spin-transfer torque causes the domain-chains to move parallel to the x axis. The colors encode the out-of-plane magnetization m_z. Red (blue) region shows m_z is positive (negative), the white area indicates the in-plane magnetization.

2. Simulation Method

Micromagnetic simulations have been done by using the public object-oriented micromagnetic framework (OOMMF)

*Project supported by the National Natural Science Foundation of China (Grant No. 11704191), the Jiangsu Specially-Appointed Professor, the Natural Science Foundation of Jiangsu Province of China (Grant No. BK20171026), and the Six-Talent Peaks Project in Jiangsu Province, China (Grant No. XYDXX-038).

†Corresponding author. E-mail: phymafs@njnu.edu.cn

© 2018 Chinese Physical Society and IOP Publishing Ltd

code at 0 K.[26] The OOMMF code has been extended to consider the Dzyaloshinskii–Moriya interaction (DMI)[27–29] and the SPC-induced magnetization dynamics by extending the Landau–Lifshitz–Gilbert (LLG) equation with additional DMI[27–29] and STT terms[7,30]

$$\frac{\mathrm{d}\boldsymbol{M}}{\mathrm{d}t} = \gamma \boldsymbol{H}_{\mathrm{eff}} \times \boldsymbol{M} + \frac{\alpha}{M_{\mathrm{s}}}\left[\boldsymbol{M} \times \frac{\mathrm{d}\boldsymbol{M}}{\mathrm{d}t}\right] - (\boldsymbol{u}\cdot\boldsymbol{\nabla})\,\boldsymbol{M} + \frac{\beta}{M_{\mathrm{s}}}\boldsymbol{M} \times [(\boldsymbol{u}\cdot\boldsymbol{\nabla})\,\boldsymbol{M}], \quad (1)$$

where the local magnetization is represented by $\boldsymbol{M}$, the effective field $\boldsymbol{H}_{\mathrm{eff}}$, the saturation magnetization $M_{\mathrm{s}} = |\boldsymbol{M}|$, the gyromagnetic ratio γ, the Gilbert damping factor α, and the nonadiabatic STT parameter β.[7,30] The effective field $\boldsymbol{H}_{\mathrm{eff}}$ is the sum of the magnetostatic, exchange, anisotropy, and Dzyaloshinskii–Moriya fields. The interfacial DMI induced Dzyaloshinskii–Moriya field is represented in the continuous form[27,28]

$$\boldsymbol{H}_{\mathrm{DM}} = \frac{2D}{\mu_0 M_{\mathrm{S}}}\left[(\boldsymbol{\nabla}\cdot\boldsymbol{m})\,\hat{z} - \boldsymbol{\nabla} m_z\right], \quad (2)$$

where D represents the continuous effective constant of DMI in the units of mJ/m^2, and the magnetic permeability is represented by μ_0, $\boldsymbol{u}$, the intensity of SPC, is defined as

$$\boldsymbol{u} = -\frac{g\mu_{\mathrm{B}}P}{2eM_{\mathrm{s}}}\boldsymbol{j}, \quad (3)$$

where g represents the Landé factor, the Bohr magnetron μ_{B}, the polarization rate of the current P, the current density $\boldsymbol{j}$, the charge of electron e charge. The electrons flow rightward in the nanotrack as shown in Fig. 1, *i.e.*, $u > 0$ means the current flows leftward in the nanotrack. It should be noted that the nucleated DCs would move along the same direction as that of the electrons propagation.

The parameters used in the simulations are those of the Co/Pt bilayer with the presence of interfacial DMI.[31] The saturation magnetization M_{s}, exchange constant A, perpendicular magnetic anisotropy K, and DMI constant D are 5.8×10^5 A/m, 1.5×10^{-11} J/m, 0.7 MJ/m^3, 3 mJ/m^2, respectively. With the application of interfacial type DMI, the domain-walls appearing in the nanotrack will be the Néel type as confirmed from the simulated magnetization. The damping constant α, non-adiabatic STT parameter β, gyromagnetic ratio γ, and polarization rate of the SPC P are 0.3, 0.3, 2.211×10^5 m/As, and 0.4, respectively. The relative value of α and β is still in debate, and which will either boost or hinder the velocity of domain-walls in nanowires.[2,7,32,33] However, the nucleation scenario of domain-chains as proposed in this work will be hardly affected by this relative value. Without loss of generality, we choose the value of $\alpha = \beta = 0.3$ (as used in Ref. [31]). The dimension of the nanotrack is 2400 nm $\times$ 60 nm $\times$ 1 nm along the x, y, and z directions, respectively. The used cells have a size of 2 nm $\times$ 2 nm $\times$ 1 nm, which is smaller than the characteristic length of material domains. There is no external magnetic fields were applied in all the simulations. For the parameters used in the simulation, $u \approx j \cdot P \cdot (4 \times 10^{-11}$ m^3/A·s), $g = 2$. The intensity of SPC is $j \approx 6.25 \times 10^{13}$ A/m^2 for $u = 1000$ m/s.

To create DCs successively, an external excitation microwave field was applied in the form of harmonic sinusoidal function $H_y(t) = H_0 \sin(2\pi f t)$ with f represents the excitation field. The microwave field with an amplitude of $\mu_0 H_0 = 5$ T is applied locally to a $\Delta x \times \Delta y \times \Delta z = 10$ nm $\times$ 60 nm $\times$ 1 nm region near the left end of the nanotrack by injecting current pulses. The magnetization in the microwave "excitation" region can be reversed locally with the formation of domains.[16] The generated domains are driven by SPC to move rightward in the nanotrack. The scenario of nucleation of N-DCs as proposed in this work, are quite related to the frequency of the excitation magnetic field f, the amplitude of the excitation magnetic field H_0, and the density of the driven spin-polarized current u. Depending on the requirement, suitable values of the three parameters can be chosen. Here, we use $u = 1000$ m/s corresponding to $j = 6.25 \times 10^{13}$ A/m^2, however, the proposed scenario can also be realized using much lower current density with the loose of the DC velocity. As shown in Fig. 1, the SPC is injected along the $-x$ direction with the electrons e move in the $+x$ direction. The DCs can only be driven to move in the nanotrack when the intensity of SPC j is larger than the threshold value $\sim 5.0 \times 10^{13}$ A/m^2. In this work, SPC with a fixed intensity, $j = 6.25 \times 10^{13}$ A/m^2, was injected. The equilibrium magnetizations profile of generated domain-chains do not relax to form equal-spaced structures when the current is switched on and off. This is attributed to the distance between neighboring "blue" domains are larger enough. Hence, the interaction between neighboring domains is weaken and avoided, and the presence of DMI will stabilize the nucleated domain-chains as well.

3. Results

Figure 1 shows the schematic diagram of the studied magnetic Co/Pt nanotrack. An antenna was applied locally on the left end of the nanotrack for generating microwave magnetic field $H_y(t) = H_0 \sin(2\pi f t)$, which will induce local magnetization reversion along with the creation of domain-chains. The nucleated domain-chains will be driven to move along the x direction by SPC-induced STT mechanism. Here, we define a single domain-chain as N-domain-chain (N-DC) if it contains N domains. As shown in Fig. 1, the period of DCs and the interval of adjacent DCs are indicated by P and S, respectively.

Figure 2 shows the serial snapshots of the nucleation process of the 2-domain-chain, which presents a sequential variation of DCs's out-of-plane magnetization m_z. A series of 2-DCs are nucleated by the locally applied excitation field $H_y(t) = H_0 \sin(2\pi f t)$ at regular time interval, with $f = 3.0$ GHz. The created 2-DCs are then driven by SPC to move rightward in the nanotrack.

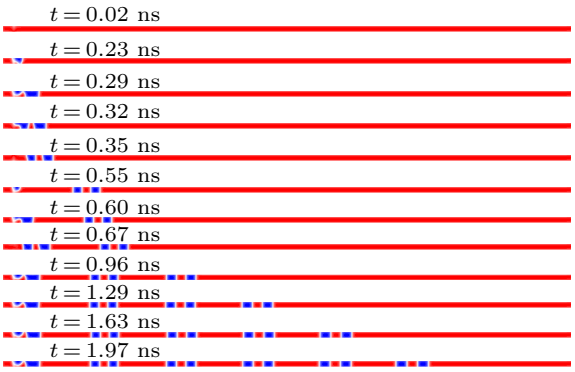


Fig. 2. (color online) Flash photographs of 2-domain-chain moving in nanotrack at specific time with $f = 3.0$ GHz, and which describes a sequential temporal evolution of the out-of-plane magnetization m_z. Red (blue) region shows m_z is positive (negative), the white area indicates the in-plane magnetization.

To understand how the frequency f of MF will affect the static properties of the DCs, we studied the temporal magnetization variation in the nanotrack with reducing f from 8 GHz to 0.5 GHz. As shown in Fig. 3, we found that the value of f affect the length N of DCs, the spacing S of adjacent DCs, and the period P of DCs. As the frequency decreases, all the number N of domains in each DC, the DC's period P and the DC's spacing S increase. For $f = 8.0$ GHz, each domain-chain contains only one domain, with $P = S$.

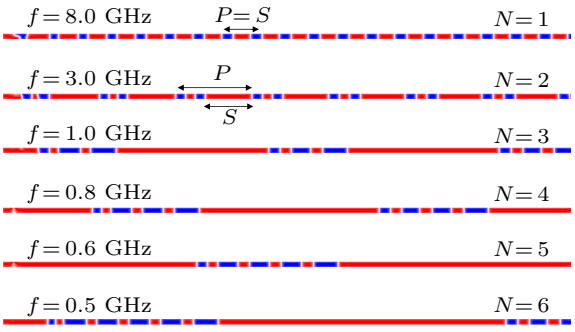


Fig. 3. (color online) Snapshot of the out-of-plane magnetization m_z for N-domain-chain under various microwave field frequency f, where N is the number of individual domains in each domain-chain.

Figure 4 describes the static properties of DCs as a function of the frequency f of the excitation MF. It can be seen that the number of domains N in each DC increases step-wisely from 1 to 13 with changing f from 11.5 GHz to 0.2 GHz. In the meantime, the DC's P and S increase with reducing f. The values of P and S are found to be inversely proportional to the value of f. Namely, the DC's characters, *i.e.*, N, P, and S, are highly dependent on the excitation MF frequency f. Hence, the static properties of the created DCs can be manipulated by controlling the excitation MF frequency f.

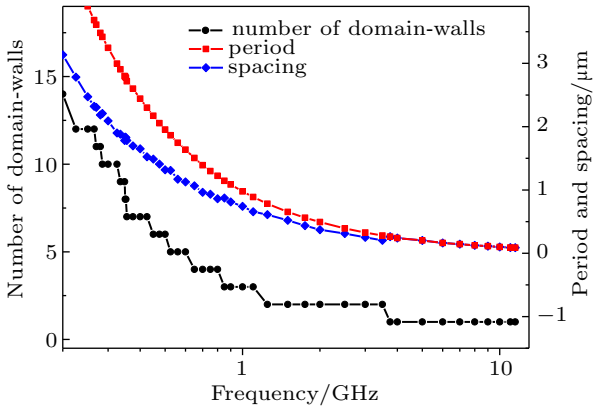


Fig. 4. (color online) The effect of excitation field frequency f on the number N of domains in each domain-chain, the special period P of domain-chains, the distance S between adjacent domain-chains.

So far, we have demonstrated the possibility of controlling DCs' properties by varying the microwave field frequency. However, the manipulation of DCs by controlling the excitation MF frequencies is not efficient from the application point of view with the requirement of excitation antenna preparation. Alternatively, with a fixed excitation MF frequency f, DCs of various properties can also be generated by temporally changing the intensity u of SPC. Figure 5(a) shows six kinds of SPC pulses, each has different temporal intensity properties $I_n(t)$. For instance, I_0 represents an SPC pulse with constant intensity $u = 1000$ m/s, while I_1, I_2, I_3, I_4, and I_5 represent the SPC pulses with temporally varied intensity, *i.e.*, SPC was switched on/off temporally. For I_1 to I_4, the current density u is switched from 1000 m/s to 500 m/s with the temporal period T_1 to T_4. Moreover, I_5 represents a more complicated case, where u varies between 1000 m/s and 500 m/s with a period T_5 (the sum of T_1, T_2, T_3, and T_4). As shown in Fig. 5(b), with only one common microwave antenna of a fixed frequency, DCs of various properties are created in the six nanotracks depending on the temporal shape of SPC pulses applied in each nanotrack. For current I_0 with a constant intensity $u = 1000$ m/s, a train of 1-DCs, are nucleated and all the nucleated domains driven into motion. In addition, the spacing S of 1-DCs can be controlled by changing the format of the SPC pulse, *i.e.*, the temporal intervals. For instance, with the SPC pulse in the form of I_1, only the domains nucleated with $u = 1000$ m/s can be driven to move along the track, while the domains nucleated with $u = 500$ m/s cannot be driven to move and annihilated at the left end of the track. Hence, as a result of domain annihilation when u is switched to 500 m/s, the created 1-DCs under I_1 has an enlarged spacing than that under I_0. Therefore, by controlling the temporal intervals of $u = 500$ m/s, the number of domains in a single chain can be

easily manipulated. As shown in Fig. 5(b), the 2-DCs, 3-DCs, and 4-DCs can be easily realized with the application of I_2, I_3, and I_4 pulses, respectively. Furthermore, a train of complex DCs, comprised of random N-DCs, can be realized through coding the temporal shape of the SPC density. For instance, a multi-DCs-train comprised of various N-DCs ($N = 1, 2, 3, 4$) can be generated with a SPC pulse in the form of I_5.

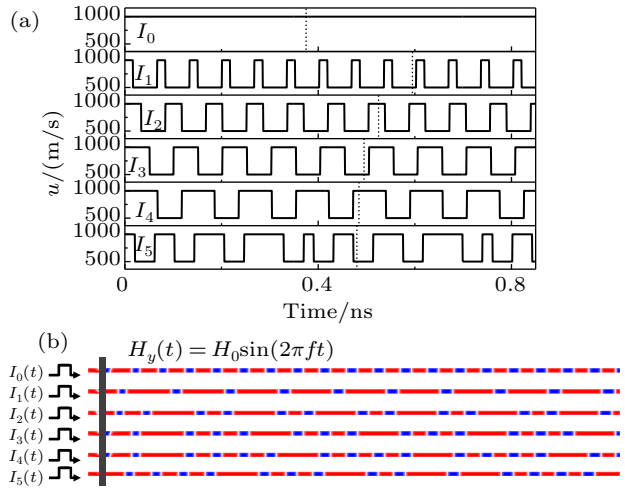


Fig. 5. (color online) Temporal modulated spin-polarized current intensity induced variation of domain-chains. (a) Intensity of SPC temporally switched on/off with $u = 1000$ m/s. (b) Flash photographs of domain-chains magnetization m_z under various SPC pulses at certain times as indicated by vertical dashed lines in (a) with $f = 8.0$ GHz.

4. Conclusion

We have numerically studied the dynamical creation of magnetic domain-chains, comprised of multi-single-domains, in magnetic nanowires. It has been demonstrated that both the frequency f of the excitation MFs and the temporal format of the SPC intensity can obviously affect the typical characteristics of generated domain-chains: the number N of individual domains in each DC, the period of DCs, and the distance between adjacent DCs. Our demonstrated scheme of multiple DCs nucleation could enrich the fields of using magnetic domains for the design of racetrack memory and logic devices.

References

[1] Li Z D, Hu Y C, He P B and Sun L L 2018 *Chin. Phys. B* **27** 077505
[2] Yuan H Y and Wang X R 2015 *Phys. Rev. B* **92** 054419
[3] Xu G Z, Xu Z, Ding B, Hou Z P, Wang W H and Xu F 2018 *Acta Phys. Sin.* **67** 137508 (in Chinese)
[4] Zhu J R, X M and Hu J G 2012 *Acta Phys. Sin.* **61** 187504 (in Chinese)
[5] Zhang Z D 2015 *Acta Phys. Sin.* **64** 067503 (in Chinese)
[6] Liu Y Z and Zang J D 2018 *Acta Phys. Sin.* **67** 131201 (in Chinese)
[7] Thiaville A, Nakatani Y, Miltat J and Suzuki Y 2005 *Europhys. Lett.* **69** 990
[8] Barnes S E and Maekawa S 2005 *Phys. Rev. Lett.* **95** 107204
[9] Wegrowe J E, Kelly D, Jaccard Y, Guittienne Ph and Ph J 1999 *Europhys. Lett.* **45** 626
[10] Vernier N, Allwood D A, Atkinson D, Cooke M D and Cowburn R P 2004 *Europhys. Lett.* **65** 526
[11] Yamaguchi A, Nasu S, Tanigawa H, Ono T, Miyake K, Mibu K and Shinjo T 2005 *Appl. Phys. Lett.* **86** 012511
[12] Tatara G and Kohno H 2004 *Phys. Rev. Lett.* **92** 086601
[13] Salhi E and Berger L 1993 *J. Appl. Phys.* **73** 6405
[14] Himeno A, Kasai S and Ono T 2005 *Appl. Phys. Lett.* **87** 243108
[15] Berger L 1984 *J. Appl. Phys.* **55** 1954
[16] Yamaguchi A, Ono T and Nasu S 2004 *Phys. Rev. Lett.* **92** 077205
[17] Boulle O, Malinowski G and Klaui M 2011 *Mater. Sci. Eng. R* **72** 159
[18] Hayashi M, Thomas L, Rettner C, Moriya R, Jiang X and Parkin S S P 2006 *Phys. Rev. Lett.* **97** 207205
[19] Grollier J, Boulenc P, Cros V, Hamzić A, Vaurès A, Fert A and Faini G 2003 *Appl. Phys. Lett.* **83** 509
[20] Kläui M, Laufenberg M, Heyne L, Backes D, Rüdiger U, Vaz C A F, Bl, J A C, Heyderman L J, Cherifi S, Locatelli A, Mentes T O and Aballe L 2006 *Appl. Phys. Lett.* **88** 232507
[21] Hayashi M, Thomas L, Rettner C, Moriya R, Bazaliy Y B and Parkin S S P 2007 *Phys. Rev. Lett.* **98** 037204
[22] Li Z and Zhang S 2004 *Phys. Rev. Lett.* **92** 207203
[23] Allwood D, Xiong G, Faulkner C C, Atkinson D, Petit D and Cowburn R P 2005 *Science* **309** 1688
[24] Allwood D A, Xiong G, Cooke M D, Faulkner C C, Atkinson D, Vernier N and Cowburn R P 2002 *Science* **296** 2003
[25] Parkin S S P, Hayashi M and Thomas L 2008 *Science* **320** 190
[26] Donahue M J and Porter D G 1999 *OOMMF User's Guide Version* 10 (Gaithersburg, MD: NISTIR 6376 National Institute of Standards and Technology)
[27] Rohart S and Thiaville A 2013 *Phys. Rev. B* **88** 184422
[28] Thiaville A, Rohart S, Jué É Cros V and Fert A 2012 *Europhys. Lett.* **100** 57002
[29] Ma F S and Zhou Y 2014 *RSC Adv.* **4** 46454
[30] Zhang S and Li Z 2004 *Phys. Rev. Lett.* **93** 127204
[31] Sampaio J, Cros V, Rohart S, Thiaville A and Fert A 2013 *Nat. Nanotechnol.* **8** 839
[32] Thomas L, Moriya R, Rettner C and Parkin S S P 2010 *Science* **330** 1810
[33] Beach G S D, Knutson C, Nistor C, Tsoi M and Erskine J L 2006 *Phys. Rev. Lett.* **97** 057203